VALIDATION OF Py-C CHEMICAL VAPOUR DEPOSITION AND INFILTRATION PROCESS CODES

F. Burgio[1*], L. Pilloni[2], M. Labanti[3], M. Scafè[1], A. Brentari[1], M. Falconieri[4], S. Sangiorgi[1]

[1] *ENEA, Faenza Technical Unit on Material Technologies, Faenza, Italy*
[2] *ENEA, Chemical and Technology Unit, Rome, Italy*
[3] *Consortium Procomp, Rotondella, Italy*
[4] *ENEA, Technical Unit on Material Technologies, Rome, Italy*
**e-mail federica.burgio@enea.it*

Keywords: CVD/CVI, pyrolytic carbon (Py-C), hydrogen concentration, process codes.

Abstract
The main purpose of the present study was to analyze the parameters controlling the Py-C CVD/CVI processes, conducted by a pilot size Isothermal/Isobaric CVI plant. In order to validate the previously developed deposition and infiltration codes [1], the experimental results and the theoretical models were taking into consideration. In particular, the effect of residence time and methane/hydrogen ratio (α) on the deposition rate and the microstructure of Py-C was investigated. Furthermore, 2D fabric preforms of carbon fibres were densified at 1200 °C by means of Py-C infiltration, varying the concentration of the gas mixture (CH_4 and H_2) and the pressure of the process.

1 Introduction

The most relevant thermo-mechanical properties of carbon - based continuous fibre ceramic composites (CFCCs) are high strength, high toughness, low weight, high reliability, thermal shock and fatigue resistance. Thanks to these special characteristics, the CFCCs are the best candidates to substitute metals and monolithic ceramics, traditionally employed for manufacturing components in energy, aeronautic, space and nuclear fields [2]. Among the techniques commonly used for the CFCCs production, chemical vapour infiltration (CVI) still represents the most significant one. Its main advantages are the versatility and the high quality of the deposits, that can be obtained under mild temperature conditions. On the other hand, this technique is quite complex, therefore the set up of all interconnected process parameters requires a long time, due to the low deposition rate [3]. Despite there has been a great interest in the CVI technique for the production of carbon - based composites (C/C_f) since the 1960s, the process has not yet been entirely understood [4]. Generally, the use of calculus codes, predicting the chemistry of the process, are expected to accelerate the parameter settings. A pilot size Isothermal/Isobaric CVI plant was developed by ENEA, to scale-up and improve a smaller laboratory CVI reactor. In particular, this contribution investigated the effects of residence time and methane/hydrogen ratio (α) on the Py-C deposition rate and microstructure. The CVD and CVI codes, previously reported by our group [1], were employed to predict the deposition and infiltration processes using experimentally derived data.

2 Experimetal

2.1 Materials and pilot plant

Graphite paper plates (85 x 40 x 3 mm) (Papyex I980 SR – Carbone Lorraine) were used as non-porous substrates for CVD tests. Graphite paper was selected thanks to its properties like chemical inertia, resistance to thermal shocks, imperviousness to hot gas, very good behaviour under vacuum conditions, as well as its ease of handling and low cost.

Preforms of PAN-based carbon fibres were used as porous substrates for CVI process. The characteristics of the C fibres were: 1.8 g/cm^3 of density, 7 μm of mean diameter and 2800 filament per yarn. The preforms, prepared stacking 8 plies of 2D plain-wave fabrics (Sigratex KDL 8003, SGL Carbon), had medium dimensions of 85x105x2 mm. The initial porosity of the preforms was about 60% and the bulk density was 0.72 g/cm^3. At the beginning, the non-infiltrated preforms were kept between two perforated graphite plates.

The carbon source gas used was methane, because its low molecular weight and small molecular dimension allow a better diffusivity [5]. Furthermore, compared to the other hydrocarbons, methane has the lower C/H ratio: the inhibiting effect of hydrogen on Py-C deposition avoids the occlusion of the superficial pores of the preforms. The methane decomposition was conducted with hydrogen, for its ability to control the carbon deposition rate [6, 7, 8], and with argon, used as carrier and purge gas. Besides, the argon produces Py-C deposits with a more uniform microstructure [9].

The processes were performed in a pilot size Isothermal/Isobaric CVI plant, designed and developed by ENEA. A schematic picture of the plant was presented in figure 1.

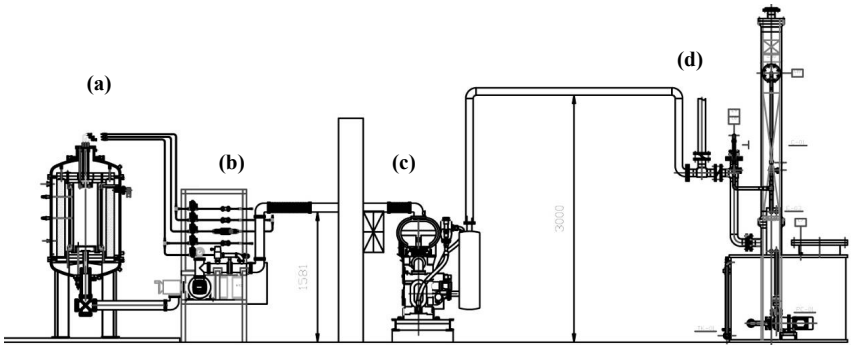

Figure 1. Layout of CVD/CVI pilot plant: (a) furnace, (b) gas inlet, (c) vacuum pumps, (d) scrubber

The vacuum furnace has an insulating liner of carbon fibre felts (Sigratherm) with effective reaction chamber dimensions of ∅300x700 mm. Gases are delivered into the reaction chamber in a top down direction and the continuous flow is obtained by means of two volumetric vacuum pumps. Graphite paper plates and preforms were positioned, on a graphite holder, at different distances from the gas inlet, 253, 375, 497 and 619 mm, respectively. All the process parameters (e.g. temperature, pressure, gas flow) and the alarm systems were controlled and acquired using a remote computer.

2.2 CVD/CVI of Pyrolytic Carbon

In order to evaluate the influence of hydrogen concentration and residence time on deposition rate and microstructure of Py-C, four Py-C CVD tests were conducted on graphite paper plates varying the process parameters: each deposition test was carried out for 20 hours at 1200 °C and 9 mbar. The procedure consisted in sample positioning, getting vacuum conditions and heating up to the process temperature. Once the temperature was stabilized, the gases were introduced into the reaction chamber. The process parameters of the four deposition tests are detailed in table 1:

Test	Q_{CH4} [sccm]	Q_{H2} [sccm]	Q_{Arc} [sccm]	Q_0 [m/s]	α	τ [s]
CVD1	1650	1450	1300	0.6	1.1	1.1
CVD2	1650	2750	0	0.6	0.6	1.1
CVD3	400	800	500	0.2	0.5	2.9
CVD4	400	1200	0	0.2	0.3	3.1

Table 1. Operating conditions of the deposition tests

were Qi, Pi, Q_0, α and τ are gas volumetric flow rate, gas partial pressure, total flow rate, methane/hydrogen ratio and residence time, respectively. The residence time τ was calculated using the equation 1:

$$\tau = \frac{V_r}{Q_0 \times \left(\frac{T}{T_0}\right) \times \left(\frac{P_0}{P}\right)} \tag{1}$$

where V_r is the reaction chamber volume, T and P are the absolute temperature and pressure values in the reaction chamber and Q_0 is the total flow rate at standard conditions T_0 and P_0.
The same procedure as CVD was used to perform the CVI experiment. Sixteen preforms, four for each distance from gas inlet, were simultaneously treated for 600 hours at 1200 °C. The CVI process was carried out with α of 0.3 and changing the operating conditions, in particular P and Qi (table 2). The process was periodically stopped to check the preform densification by mass gain, porosity and SEM measurements.

Infiltration Step	P [mbar]	Q_{CH4} [sccm]	Q_{H2} [sccm]	α
CVI1: 0 ÷ 300h	9	400	1200	0.3
CVI2: 300 ÷ 350 h	19	400	1200	0.3
CVI3: 350 ÷ 600 h	18	800	2400	0.3

Table 2. Operating conditions of the CVI experiment

2.3 Characterizations

In CVD experiments, steady-state deposition rates ($R_{deposition}$) of pyrolytic carbon were determined by the mass gain of the substrates after deposition time of 20h, using equation 2:

$$R_{deposition} = \frac{\left(m_f - m_i\right)}{A_s \times t \times \rho} \tag{2}$$

where m_i and m_f are the mass of the samples before and after the deposition, A_s is the superficial area of the samples, t the duration of the deposition and ρ the density of Py-C.
In CVI experiment, the initial density and porosity of the preforms were obtained from the fibre volumetric fraction (0.4) and the fibre density (1.8 g/cm^3). Periodically, the process was stopped and, for each gas inlet distance, samples were sliced from the infiltrated preforms, in order to monitor their density and open porosity. The geometrical density of each sample was calculated from its weight and dimensions. The open porosity was evaluate following the equation 3:

$$P\% = \left[V_{total} - \left(V_{fibre} + V_{matrix}\right)\right] / V_{total} \times 100 \tag{3}$$

were V_{total} is the geometric volume of the sample and $V_{fibre} + V_{matrix}$ is the volume obtained with helium pycnometer (AccuPyc 1330 Pycnometer – Micromeritics). These values of density and porosity were taken as the average ones of the composites obtained in each position.
The infiltration progressing was also evaluated measuring the Py-C thickness, deposited on the inner and outer fibres of the preforms, by SEM images (SEM Leo 438 VP equipped with EDS – Link ISIS 300). The Py-C thickness was also used to evaluate the steady-state deposition rate. A preliminary study of the Py-C microstructure, obtained both in CVD and in CVI experiments, was carried out by Raman analysis. The Raman spectrometer is based on a 550 nm triple grating monochromator (Jobin-Yvon TRIAX 550) coupled to a liquid nitrogen cooled CCD detector. The optical sampling head is a home-built micro-Raman setup equipped with a 532 nm laser excitation light focused to a 3 micron spot onto the sample

2.4 Process modelling
The modelling of the carbon deposition process was performed using a literature model, that describes the methane pyrolysis by 36 chemical reactions and reports the related reaction rates [10]. The total porosity of the composites was evaluated by literature statistical models [11, 12, 13]: the obtained data were used for the modelling of the infiltration process. The simulation of the processes was conducted using a computational tool (Mathematica) and the CVD and CVI codes, previously presented [1].

3 Results

3.1 Influence of hydrogen concentration and residence time
The experimental results concerning the influence of hydrogen concentration on the Py-C deposition rate are presented in figures 2 and 3. The influence was investigated keeping unchanged total flow rate and residence time, but with different α values: the methane/hydrogen ratio was varied changing only the hydrogen concentration. It was evidenced that a higher hydrogen concentration inhibited the Py-C deposition rate only at low flow rate (0.2 m/s). Instead at higher flow rate (0.6 m/s), the hydrogen influence was not evident: the deposition rates obtained with α of 1.1 and 0.6 were comparable. This behaviour can be ascribed to the fact that at high flow rates, so at low residence time, the hydrogen has no sufficient time to react and form the superficial species that inhibit the Py-C deposition. Furthermore, it has been observed that higher residence time resulted in a more homogeneous deposition profile, along the axis of the reaction chamber.

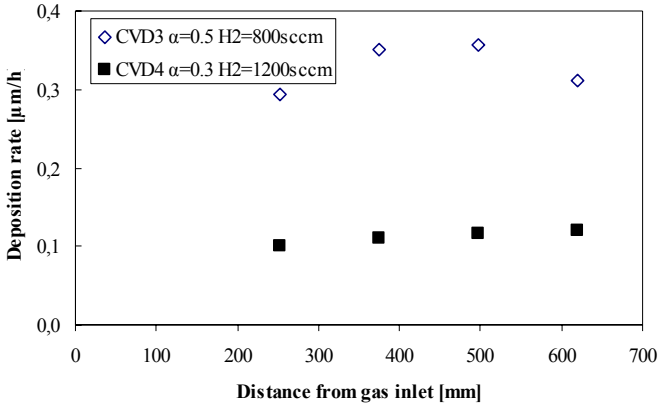

Figure 2. Py-C deposition rate *vs* distance from gas inlet (Q_0=0.2 m/s, τ=3 s, Q_{CH4}=400 sccm)

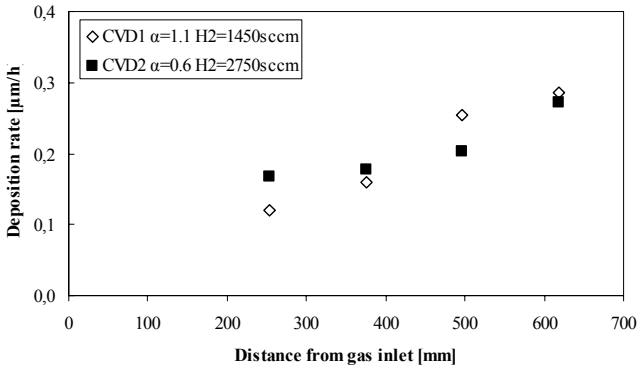

Figure 3. Py-C deposition rate vs distance from gas inlet (Q_0=0.6 m/s, τ=1 s, Q_{CH4}=1650 sccm)

The influence of residence time on Py-C deposition rate is shown in figure 4, where the deposition rates were compared, at similar values of α, varying the flow rate of the gases and τ. Figure 4 shows that the lower the residence time, the lower the Py-C deposition rate, despite the much higher flow rate of methane used. Also in this case, the deposition profile resulted more homogeneous with a high residence time.

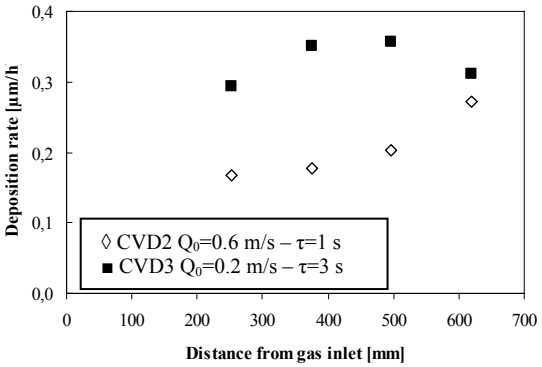

Figure 4. Py-C deposition rates *vs* distance from gas inlet at various operating conditions: (◊ CH_4=1650sccm, H_2=2750sccm, α=0.6) and (■ CH_4=400sccm, H_2=800sccm, α=0.5)

The effect of both hydrogen concentration and residence time on Py-C microstructure was investigated by Raman analysis. The micro laser Raman spectroscopy was carried out on the samples used for the four CVD tests. The Raman spectra obtained were similar for each experiment (figure 5): a qualitative comparison with literature data indicated a Py-C Rough Laminar microstructure [14, 15].

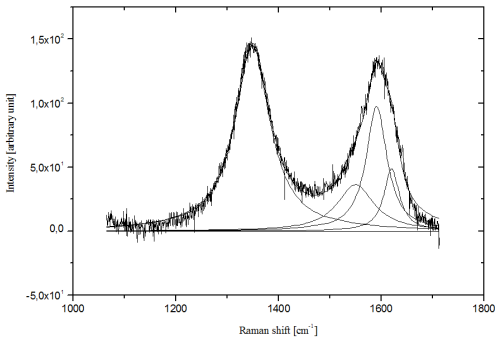

Figure 5. Raman spectrum of the Py-C deposited

3.2 Densification behaviour of C/Cf composites

The CVI process was started by choosing the operating conditions of the CVD4 test, because of the low deposition rate (0.1 μm/h) and the homogeneous profile (infiltration step CVI1). However, after infiltration time of 300 hours, the densification degree was insufficient: the composites had a porosity of about 30% (figure 6).

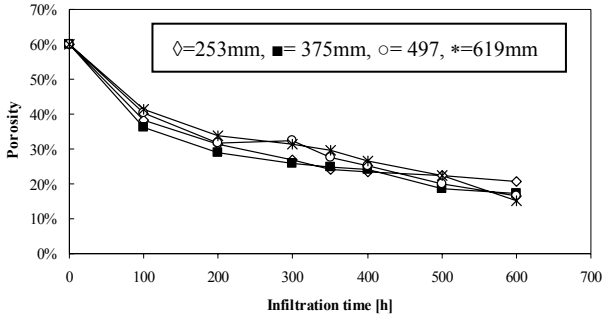

Figure 6. Porosity of the composites as a function of the infiltration time at different distance from gas inlet

Therefore, in order to raise the deposition rate, the pressure was increased up to 19 mbar (infiltration step CVI2). The increase of the pressure didn't determine a significant rise in the deposition rate (from 0.05 to 0.08 μm/h), as deduced from the SEM measures of the Py-C deposit thicknesses (figure 7). The infiltration step CVI3, between 350 and 600 hours, was carried out keeping constant α and total flow rate, but with higher hydrogen and methane concentrations than the previous step: the deposition rate was about 0.2 μm/h (figure 7).

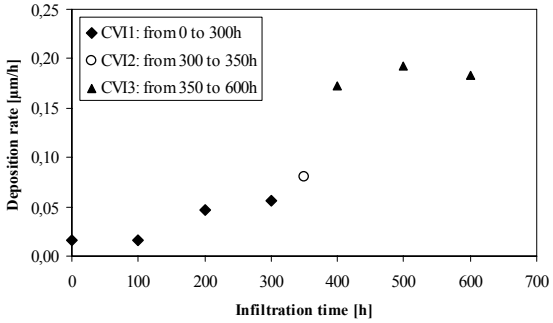

Figure 7. Deposition rate, obtained from the SEM measures of the Py-C deposit thickness, as a function of the infiltration time at different operating conditions

The obtained value of deposition rate, allowed a progressive infiltration of the preforms without occluding the outer pores, as shown by the SEM images (figure 8). This behaviour was also evidenced by the continuous increase of the composite bulk density (figure 9). Furthermore, the densification behaviour of the composites through the furnace chamber was rather homogeneous (figure 9). The C/C_f produced after 600 hours of infiltration were characterized by a medium bulk density of 1.3 g/cm^3 and a residual porosity of about 17%.

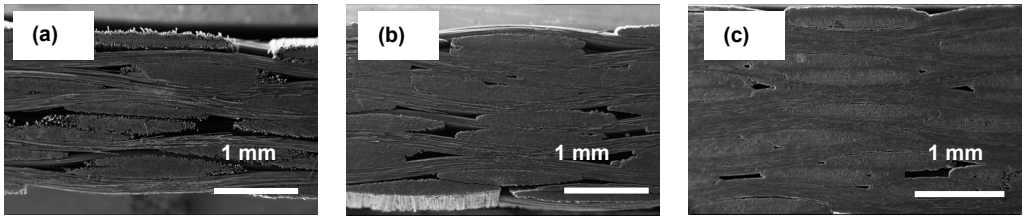

Figure 8. SEM images of the composite sections with increasing infiltration time (a) 100h, (b) 200h, (c) 300h

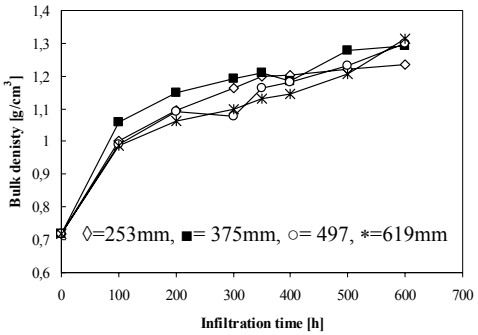

Figure 9. Bulk density of the composites *vs* infiltration time at different distance from gas inlet

3.3 Validation of process codes

The integration of the model provided the concentration profiles of the chemical species along the furnace axis: it was evidenced that the chemical species responsible of the carbon deposition are $\cdot CH_3$ and $\cdot C_2H$, with the following heterogeneous chemical reactions:

$$\cdot CH_3 \leftrightarrows C_{sol} + 3H\cdot \quad (4) \qquad \cdot C_2H \leftrightarrows 2C_{sol} + H\cdot \quad (5)$$

Using the Py-C deposition rates, experimentally obtained varying the methane/hydrogen ratio in the CVD tests, the chemical rates of the equations 4 and 5 were estimated (equations 6-9).

T<1100°C

$$K_4^+ = 0.5563 \times e^{\left(-11838/T\right)} \qquad K_4^- = 4399 \times 10^{18} \times e^{\left(-69427/T\right)} \quad (6)$$

$$K_5^+ = 3.9057 \times 10^{22} \times e^{\left(-82396/T\right)} \qquad K_5^- = 2.9885 \times 10^{14} \times e^{\left(5171.4/T\right)} \quad (7)$$

T>1100°C

$$K_4^+ = 3.0988 \times 10^{13} e^{\left(-58100/T\right)} \qquad K_4^- = 3.9262 \times e^{\left(-6201.6/T\right)} \quad (8)$$

$$K_5^+ = 1.8726 \times 10^{-9} \times e^{\left(-23941/T\right)} \qquad K_5^- = 2.5268 \times 10^{6} \times e^{\left(-20555/T\right)} \quad (9)$$

The simulated and experimentally measured deposition rates, obtained in CVD tests with different α, were compared (not shown). The deposition rates calculated with the CVD code fitted to the experimental data except for α 0.3: for this value the deposition rates resulted underestimated. The deposition rates so obtained, describing also the hydrogen effect, were used in the CVI code to check the accordance between predicted and experimentally derived data. In particular the evolution of the bulk density of the ceramic preform, placed at 375 mm from the gas inlet, was evaluated for the infiltration step CVI1 (figure 10). The mismatch between experimentally measured and simulated density, in the first hours of infiltration, is probably due to the effects of preform specific surface. After 100 hours of infiltration, the CVI code simulated the experimental density with an error of about 10%.

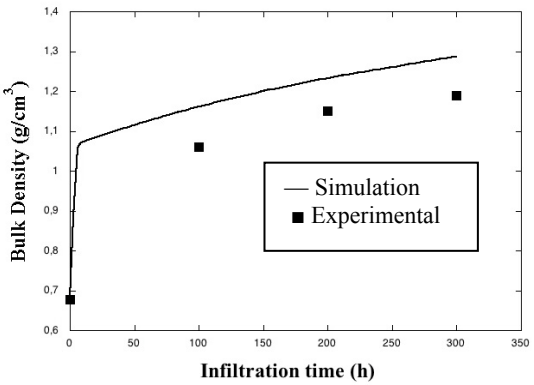

Figure 10. Comparison of model predictions (lines) with experimental (symbols) bulk density

4 Conclusions

The study of the parameters controlling the CVD process indicated that the residence time was the key factor: the influence of a higher hydrogen concentration on retarding the pyrolytic carbon deposition was evident only at high residence time. Furthermore, it has been shown that the residence time affects the homogeneity of the deposition profile along the reaction chamber: the deposition profile resulted more homogeneous with high residence time. However, in the specific operating conditions here discussed, there was no evidence of the influence of residence time and hydrogen concentration on the microstructure of the Py-C. Regarding the infiltration process, the C/C_f produced had a density and an open porosity lower than those expected for a C/C_f with good mechanical properties: these results were attributed to the low deposition rate used for the first 300 hours of densification process.
The deposition rates simulated by CVD code fitted to data experimentally obtained, except for α 0.3: for this value the deposition rates resulted underestimated. In the case of CVI process, the effects of specific surface on the Py-C deposition rates determined a mismatch between experimentally obtained and predicted density data, especially in the first hours of infiltration process. Therefore, the CVD and CVI models accounted for the inhibiting effects of hydrogen on carbon deposition, but it will be necessary to modify the reaction rates and better investigate the effects of the specific surface in order to improve the accuracy of the models.

References

[1] Burgio F., Pilloni L., Labanti M., Scafè M., Brentari A., Sangiorgi S. *Development of C_f/C composites by CVI technology: validation of process codes* in "Proceeding of *7th International Conference on High Temperature Ceramic Matrix Composites HTCMC"*, Bayreuth, Germany, (2010).
[2] Taylor R. *Carbon Matrix Composites* in "Comprehensive Composites Materials", edited by Kelly A. and Zweben C. Elsevier, **4**, pp. 387-426 (2000).
[3] Naslain R. Design, preparation and properties of non-oxide CMCs for application in engines and nuclear reactors: an overview, *Composites Science and Technology*, **64**, pp. 155-170 (2004).
[4] Li A., Norinaga K., Zhang W., Deutschmann O. Modeling and simulation of materials synthesis: Chemical vapor deposition and infiltration of pyrolytic carbon. *Composites Science and Technology,* **68**, pp. 1097–1104 (2008).
[5] Benzinger W., Huttinger K.J. Chemical vapour infiltration of pyrocarbon: I. some kinetic considerations. *Carbon*, **34**, pp. 1465-1471 (1996).
[6] Becker A. Chemistry and Kinetics of Chemical Vapor Deposition of Pyrocarbon – IV Pyrocarbon Deposition From Methane In The Low Temperature Regime. *Carbon*, **36**, pp. 213-224 (1998).
[7] Oberlin A. Review – Pyrocarbon. *Carbon,* **40**, pp 7-24 (2002).
[8] Becker A. A hydrogen inhibition model of carbon deposition from light hydrocarbons. *Fuel*, **79**, pp. 1573-1580 (2000).
[9] Pierson H. O. The Chemical Vapor Deposition of Carbon on Carbon Fibers. *Carbon*, **13**, pp. 159-166 (1975).
[10] Holmen A. Pyrolysis of natural gas: chemistry and process concepts. *Fuel Process. Tech.*, **42**, 249 – 267 (1995).
[11] Burganos V.N. Knudsen diffusion in parallel, multidimensional or randomly oriented capillary structures. *Chem. Eng. Science*, **44**, 2451 – 2462 (1989).
[12] Melkote R.R. Gas diffusion in random-fiber substrates. *AIChE Journal*, **35**, pp. 1942 – 1952 (1989).
[13] Tomadakis M. Effective Knudsen diffusivities in structures of randomly overlapping fibers. *AIChE Journal*, **37**, 74 – 86 (1991).
[14] Bourrat X., Fillion A., Naslain R., Chollon G., Brendle M. Regenerative laminar pyrocarbon. *Carbon*, **40**, pp. 2931–2945 (2002).
[15] Vallerot J. M., Bourrat X., Mouchon A., Chollon G. Quantitative structural and textural assessment of laminar pyrocarbons through Raman spectroscopy, electron diffraction and few other techniques. *Carbon*, **44**, pp. 1833–1844 (2006).